Spectrochimica Acta Part A: Molecular and Biomolecular Spectroscopy 254 (2021) 119627

Contents lists available at ScienceDirect

Spectrochimica Acta Part A: Molecular and Biomolecular Spectroscopy

journal homepage: www.elsevier.com/locate/saa

Development of a novel NIR viscosity fluorescent probe for visualizing the kidneys in diabetic mice

Lixuan Dai [a], Mingguang Ren [a,b], Weiying Lin [a,c,*]

[a] Institute of Fluorescent Probes for Biological Imaging, School of Chemistry and Chemical Engineering, School of Materials Science and Engineering, University of Jinan, Jinan, Shandong 250022, China
[b] State Key Laboratory of Biobased Material and Green Papermaking, Shandong Academy of Sciences, Qilu University of Technology, Jinan 250353, China
[c] Guangxi Key Laboratory of Electrochemical Energy Materials, Institute of Optical Materials and Chemical Biology, School of Chemistry and Chemical Engineering, Guangxi University, Nanning, Guangxi 530004, China

HIGHLIGHTS

- **NI-VD** visualized and proved the distinction diabetic kidney for the first time.
- **NI-VD** has maximum emission peaks at 730 nm with a large Stokes-shift.
- **NI-VD** can accurately target with mitochondria.
- **NI-VD** can detect changes in viscosity in a complex cellular environment.

GRAPHICAL ABSTRACT

We report a novel probe that can visualize the distinction diabetic kidney from normal kidney for the first time by monitoring changes in cell viscosity. The synthesis method of **NI-VD** is simple and feasible. The large Stokes' shift, near-infrared emission peak, and specific response imply that **NI-VD** can monitor changes in mitochondrial viscosity at the cell, organ, and organism level. **NI-VD** is a new solution for the diagnosis and treatment of diabetic nephropathy.

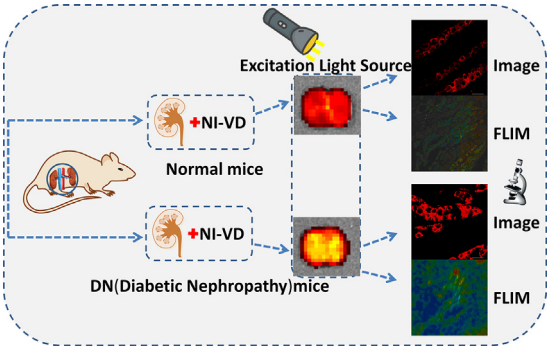

ARTICLE INFO

Article history:
Received 23 December 2020
Received in revised form 22 January 2021
Accepted 9 February 2021
Available online 26 February 2021

Keywords:
Fluorescent probe
Mitochondria
Viscosity
Visualization
Diabetic nephropathy

ABSTRACT

Viscosity is an important parameter for evaluating cell health, and abnormal viscosity can cause a variety of intracellular organelle function disorders. The mitochondria are a key organelle in cells, and the viscosity of the mitochondria determines the state of the cell. In this work, we report a novel near-infrared fluorescent probe, referred to as **NI-VD**, that has a large Stokes-shift and a satisfactory response multiple. **NI-VD** can sensitively detect changes in cell viscosity in cells and tissues, and it can effectively avoid interference from the overlap of excitation and emission light. The fluorescence spectrum shows that **NI-VD** has maximum emission peaks at 730 nm, and the fluorescence intensity is amplified with an increase in the solution viscosity. The response from pure PBS solution to glycerol changes by 13-fold. After confirmation in a variety of cell and biological models, **NI-VD** can detect the changes in viscosity in mitochondria. Most importantly, this study is the first to visualize the differences between the kidneys of diabetic mice and normal mice. This approach is a new solution for the diagnosis and treatment of diabetic nephropathy.

* Corresponding author.
E-mail address: weiyinglin2013@163.com (W. Lin).

https://doi.org/10.1016/j.saa.2021.119627
1386-1425/

1. Introduction

Cells are as precise as machines, where each organelle plays a unique function. There are many essential factors that ensure that normal physiological activity can be maintained in cells such as ROS, RNS, small molecular thiols, and viscosity [1–7]. At the microscopic level, viscosity is key to diffusion control and plays a significant role in the chemical behavior and biological behavior. Some normal chemical and biological activities including signal transmission, protein folding, and enzyme catalysis work on the basis of viscosity balance. Studies have shown that abnormal activities are usually caused by abnormal changes in viscosity in cells. Consequently, viscosity is an important indicator of healthy cells.

The viscosity of cells is 1–2 cP, but it can significantly increase in diseased cells reaching 140 cP and even more [8–11]. At the macroscopic level, the normal activities in different organelles like mitochondria are affected by viscosity. There can be poor organelle performance when the viscosity is out of range. Many common diseases such as diabetes, Alzheimer's disease, and neurodegenerative diseases all feature abnormal cell viscosity [12,13].

Mitochondria dominate many cellular processes include ATP production, central metabolism, and apoptosis [14–16]. Some common functions of mitochondria will be inhibited by the alteration in mitochondrial membrane fluidity including a reduction in the electron transport chain activation, and release of cytochrome *c* [17]. Therefore, for better medical care, it is important to monitor the viscosity in the mitochondria.

Drop ball, capillary, and rotational viscometers are traditional viscosity measurement methods, but these methods cannot make measurements at the cell level or in vivo [18–20]. Fluorescent probes offer low phototoxicity, deep penetration, and high-resolution biological imaging. They can measure changes in the microenvironment of subcellular regions. After a long period of development, the molecular rotor is still an important method for studying the viscosity of cells [21–23]. The rotation of the molecular rotor is not inhibited in a low-viscosity environment. Faster rotation relaxes the excitation energy with little fluorescence. Rotation is hindered in a high-viscosity environment such as glycerol, thus reducing the possibility of non-radiating pathways: This increases the fluorescence. In recent years, many rotor probes have emerged, and some of them have been successfully applied to detect changes in the viscosity of cells in organisms. However, most of the reported probes have two major shortcomings: One problem is the emission wavelength of probe is too small and not in the near-infrared region. The second is that the Stokes-shift is not long enough to prevent an overlap in excitation light and emission light—thus, there is autofluorescence and a high background.

Diabetes is a keystone disease with many related diseases. Diabetic nephropathy (DN) is a common complication. Little is known about the mechanism and specific function and injury in vascular endothelial cells after diabetes induction. A close relation has been seen between the complications of diabetes (such as vascular complications) and dysfunction of mitochondria in vascular endothelial cells [24–27]. In the kidney, the glomerular vascular endothelial cells are in a state of diabetic hyperglycemia for a long time, and glucose metabolic disorders will appear in cells with this situation. More reactive oxygen species (ROS) are produced in the mitochondria in this situation. These undesirable changes will lead to an increase in the permeability of the mitochondrial outer membrane and can even lead to glomerular endothelial cell apoptosis and tissue damage [28,29]. However, the present research by fluorescence probe that can distinguish between abnormal diabetic kidneys and normal kidneys is still vacant.

Our previous studies showed that the production of reactive oxygen species (ROS) increases with abnormal mitochondrial viscosity [30,31]. We developed a novel near-infrared probe, **NI-VD**, that belongs to the classic molecular rotor probe. The classic fluorophore phenolic dihydroxanthene is used as the main body of the probe. It is easy to modify and synthesize [32]. We introduced a methoxy electron-donating group to improve its structure-activity relationship. Quinoline is the positioning group of mitochondria—it locates the negative potential on the inner mitochondrial membrane with a positive charge on N and also extends the conjugate structure to obtain a larger emission wavelength [33–35]. **NI-VD** has weak fluorescence in low-viscosity solutions and strong fluorescence in high-viscosity solutions. The maximum emission of **NI-VD** is 740 nm with a maximum response multiple of 13-fold. It can sensitively monitor viscosity changes in living cells. The background fluorescence interference during the imaging process is minimal and benefited from a large Stokes' shift. We also used fluorescence lifetime imaging microscopy (FLIM) to confirm our experimental results, fluorescence lifetime is a stable physical property of fluorophores [36]. **NI-VD** can measure the kidneys of diabetic mice and normal mice for the first time.

2. Experimental section

2.1. Synthesis

Twisted internal charge transfer (TICT) is a classic mechanism for designing small molecule fluorescent probes that respond to viscosity. Molecules devised by TICT usually have "D-π-A" molecular configuration, and a strong electron withdrawing group is used for the acceptor. The donor was a strong electron donor. Scheme 1 shows that the two parts of **NI-VD** were linked though a flexible-conjugated linker. Phenolic dihydroxanthene with a methoxy was the donor, and quinolone was the acceptor, meanwhile, the quaternary ammonium salt group makes **NI-VD** water soluble and helps **NI-VD** target mitochondria. The Structural characterization data, including ^{1}H NMR, ^{13}C NMR and HR-MS (High Resolution Mass Spectrometry) were provided in Supporting Information.

NI-VD exhibits weak fluorescence in low-viscosity solutions because the solvent cannot prevent the rotor from rotating freely through the single bond. In high-viscosity solutions, the rotation of the rotor was restrained, and the energy tend to return to the ground state in the form of a radiative transition; thus, it has strong fluorescence. Furthermore, the structure of a large conjugate chain gives **NI-VD** a longer emission wavelength and lower background fluorescence.

2.2. Synthesis of the compound ***NI-VD***

Compounds 1 and **2** were prepared as described [32,37]. **Compound 1** (0.5 g) and **Compound 2** (1 g) were mixed in ethanol and added to a dry clean round bottom flask. A drop of piperidine was carefully added. The reaction was allowed to proceed. We used TLC to monitor the progress; during the reaction, the temperature was held at 50 °C. After the reaction was completed, the solvent was removed by evaporation under reduced pressure. We purified the remaining residue using column chromatography on a silica gel. The polarity of the solvent is "CH_2Cl_2/methanol" = 50: 1, v/v. The product was a purple powder (600 mg, 38% yield). ^{1}H NMR (400 MHz, $CDCl_3$ and CD_3OD) δ 9.70 (d, 1H), 8.63 (d, 1H), 8.49 (d, 1H), 8.36 (d, 1H), 8.06 – 7.98 (m, 2H), 7.85 – 7.80 (m, 1H), 7.18 – 7.06 (m, 3H), 6.78 – 6.72 (m, 2H), 4.56 (s, 3H), 4.02 (s, 3H), 2.69 (dt, 4H), 0.89 (d, 2H). ^{13}C NMR (151 MHz, $CDCl_3$ and CD_3OD) δ 161.90, 155.61, 154.14, 153.82, 145.46, 139.23, 138.44, 134.52, 128.37, 127.46, 127.21, 127.12, 126.10, 125.59, 118.09, 115.36, 113.39, 112.90, 112.51, 111.03, 100.31, 55.13, 43.19, 29.18, 24.47,

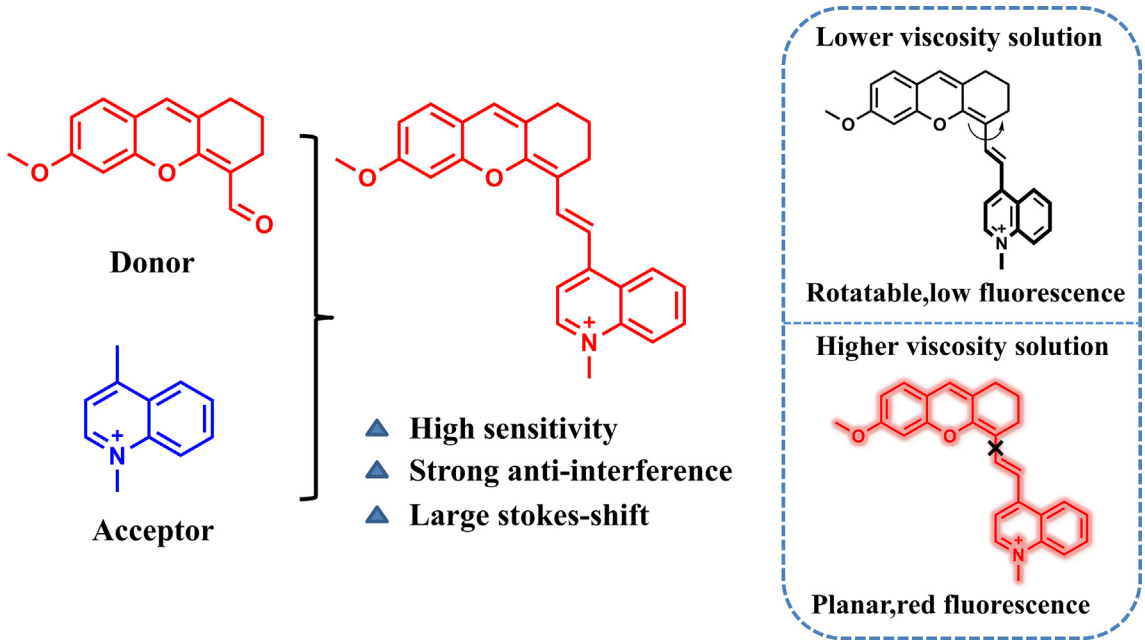

Scheme 1. Design of near-infrared emission fluorescent viscosity probe **NI-VD**.

20.63. HRMS (ESI): *m/z* calculated for $C_{26}H_{24}NO_2^+$: 382.1806 [M] $^+$, found: 382.1804

2.3. Optical studies

The reagents and medicines used in this experiment are all taken from the supplier and used directly without further processing. In addition, the water used in the whole process of experiment was distilled water that has been purified twice. The instrument used in this experiment is not different from the instrument used in the previous work.

2.4. Cells culture

HeLa cells, HepG2 cells were cultured in culture medium (DMEM mixed with 10% fetal bovine serum). All the above cells were cultured under the environment that 95% air blended with 5% CO_2 at 37 °C.

2.5. Cytotoxicity assay

This experiment uses the colorimetric methyl thiazolyl tetrazolium (MTT) widely applied in biology to test the toxicity of the **NI-VD** to cells. Dispersed the HeLa or HepG2 cells in the culture medium (Dulbecco's modifed eagle medium supplemented with 10% fetal bovine serum and 1% penicillin/streptomycin) evenly, placed the cells in an equal amount on a 96-well plate carefully, and incubated overnight at 37 °C and 5% CO_2 atmosphere for overnight. After the cells were completely attached to the bottom of the 96-well plate, replace the original culture medium with a medium containing a series of concentrations of **NI-VD** (0, 1, 2, 3, 5, 10, 20 μM) and continue to culture for 24 h. Next step was washed cells by PBS Buffer, and inject 500 μL of culture medium into the 96-well plate as before. Furthermore, use 50 μL MTT (5 mg/mL) to label the cells for 4 h in each well. Subsequently, remove all the culture medium, use the principle that violet formazan could be dissolved in water-DMF mixture, add it in each well and mix well. Finally, absorbance of the solution was measured at 730 nm using a microplate reader. The cell viability was determined by assuming 100% cell viability for cells without **NI-VD**.

2.6. Fluorescence lifetime imaging with *NI-VD* in kidney

Part of the fluorescence lifetime experiment was measured at Experimental Center, Shandong University of Traditional Chinese Medicine, Ji'nan, China. The instruments used are freezing microtome (Leica CM1950), inverted-type laser scanning confocal microscope (Zeiss LSM880 NLO). Soak the freshly kidneys from two groups of mouse in PBS solution containing **NI-VD** (15 μM), After 30 min marking with **NI-VD**, the samples were made into sections with a thickness of 20 μm using a freezing microtome, and the sections were placed on a cover glass. Place the sample on the glass slide and observe under the microscope.

3. Results and discussion

3.1. Spectroscopic properties toward viscosity

We next tested and recorded the spectral properties of **NI-VD**. There are few organic solvents in biology, and we used phosphate buffer saline and glycerin as control samples. Fig. 1**a** shows that the probe has an absorption peak at 550 nm in the low-viscosity pure PBS solvent. This peak redshifts to 617 nm when the solvent is pure glycerol. This confirms that **NI-VD** can be a rotor probe for viscosity. We next evaluated the relationship between the emission and viscosity of **NI-VD** in glycerol and PBS solutions prepared with different volume ratios. The fluorescence emission spectrum is the next item to be tested. A 10-fold increase was seen in the fluorescence emission spectrum (Fig. 1**b**). It is increased with changes in viscosity from 1.6 cp to 563.6 cp. At the same time, the quantum yield increased from PBS (Φ_f = 0.28%) to glycerol (Φ_f = 3.67%) with an increase in viscosity and fluorescence intensity. After testing, there is a good linear relationship between the fluorescence lifetime and the change in viscosity. The correlation coefficient from the two groups was studied via the Förster–Hoffmann equation—the probe can be used to measure viscosity.

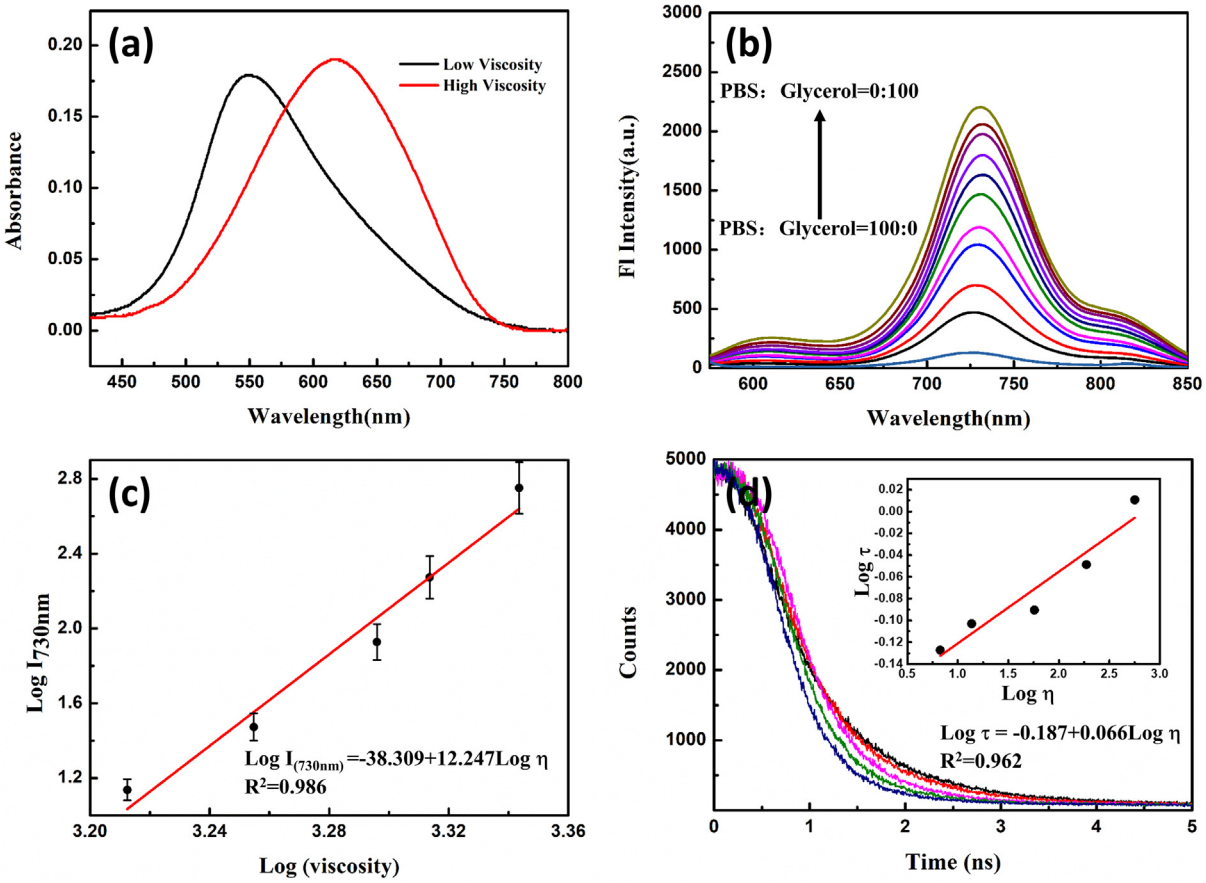

Fig. 1. (a) UV–Vis spectra of **NI-VD** (10 μM) in PBS and glycerol. (b) Fluorescence spectra of 10 μM **NI-VD** in PBS – glycerol systems at various ratios (λ_{ex} = 520 nm). (c) Linear relationship between log I_{730} and log η, R^2 = 0.986, x = 12.247. (d) Fluorescence lifetime spectra of **NI-VD** under different solution viscosities in the PBS/glycerol system. (λ_{em} = 535 nm). Inset: the linear relationship between log τ and log η.

3.2. Solvent effect

A theoretical calculation of **NI-VD** suggested that as the dihedral angle increases from 0°, the corresponding energy becomes higher and higher until it reaches a maximum value of 100°. The energy will gradually decrease until it is 180° as the C-C single bond continues to rotate (Fig. S1, ESI†). This is a typical feature of TICT. The lowest energy configuration of **NI-VD** is when the dihedral angle is 0°; this is also the configuration that is ultimately maintained in a high-viscosity solution.

Feature of ICT is the solvent effect, so as in TICT. The spectrum will red-shift as the solvent polarity decreases. We tested the absorption and fluorescence spectra of probes in non-polar solvents (Fig. S2, ESI†); the results were as expected.

3.3. Anti-interference and selectivity

To study the specificity of the probe's response to viscosity, we selected some common interfering ions and molecules in organisms and added these ions to high-viscosity and low-viscosity solvents for detection [38,39]. These ions and molecules include reactive nitrogen species (RNSs), reactive oxygen species (ROSs), metal ions, and small molecule mercaptans: GSH, H_2O_2, DBTP, HClO, Cys, $NaHSO_3$, $NaNO_3$, TBHP, O^{2-}, Mn^{2+}, Cu^{2+}, Fe^{2+}, NH_4F, $NaNO_2$, OH^-, $Na_2S_2O_3$, Ag^+, Zn^{2+}, Al^{3+}, and Mg^{2+} [40]. The results show that the addition of these interfering ions and molecules only causes small changes to the fluorescence intensity of the probe (Fig. 2). In this experiment, **NI-VD** showed an excellent specific response to viscosity.

The pH value of the cell microenvironment is about 7.4 [41]. Therefore, to verify that **NI-VD** can monitor the viscosity stably

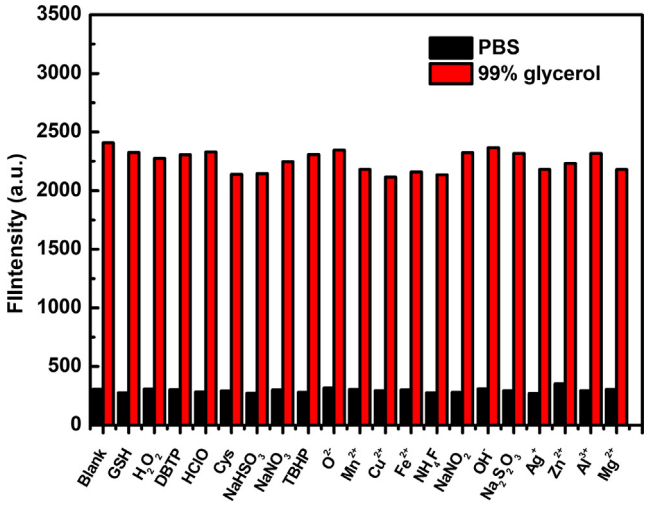

Fig. 2. Fluorescence intensity at 730 nm of **NI-VD** (10 μM) treated with various species in PBS and 99% glycerol solution after 30 min at room temperature (1 to 21 are reference to blank, GSH, H_2O_2, DBTP, HClO, Cys, $NaHSO_3$, $NaNO_3$, TBHP, O^{2-}, Mn^{2+}, Cu^{2+}, Fe^{2+}, NH_4F, $NaNO_2$, OH^-, $Na_2S_2O_3$, Ag^+, Zn^{2+}, Al^{3+}, Mg^{2+}. The concentration of each type of interfering ion is 20 μM).

in the appropriate pH range, we conducted stability experiments including pH stability (Fig. S3, ESI†) and light stability (Fig. S4, ESI†). The results show that the probe can respond viscosity in a stable way over a broad pH range of 3 to 9. All of the testing revealed that **NI-VD** has value in complex environments such as living organisms.

3.4. Fluorescence imaging of *NI-VD* in living cells

Combining the above experiments with the excellent performance of **NI-VD** and its emission in the near-infrared region, we further explored its value in monitoring viscosity. First, we performed an MTT experiment; the cytotoxicity assay results show that the low-dose probe had minimal effects on HeLa cells and HepG2 cells (Fig. S5, ESI†). The next step is to perform a colocalization experiment with commercial dye Mito-Tracker Red. The results shown that **NI-VD** can penetrate into HeLa and HepG2 cells. It locates in the mitochondria specifically. The fluorescence of Mito-Tracker Red was observed in the green channel, and the fluorescence of **NI-VD** was displayed in the red channel. There was strong consistency in scatter plots of the two. Pearson coefficients were used to represent the correlation and reached 0.89 and 0.93 for HeLa and HepG2 cells, respectively (Fig. S6, ESI†). This means that **NI-VD** could locate mitochondria specifically and monitor the viscosity of mitochondria in cells.

3.5. Monitoring of viscosity changes in living cells

An abnormal viscosity can indicate cellular disease. Thus, considering that **NI-VD** localizes to the mitochondria, we used monensin and nystatin to build a cell model of disease. Monensin and nystatin induce dysfunction of mitochondria in the cells based on mitochondrial swelling [42,43]. We monitored the change in mitochondrial viscosity (Fig. 3). After HeLa cells were incubated with **NI-VD** for 30 min, only weak red fluorescence was seen in the mitochondria of normal HeLa cells. The cells were then treated with nystatin (10 μM) and monensin (10 μM) for 30 min before being treated with **NI-VD**. There was obvious swelling from the mitochondria; intense fluorescence of mitochondria appeared at the same time. The spherical morphology of mitochondria in the cell can be explained by the stimulation of monensin and nystatin. We did the same experiment on HepG2 cells and observed similar phenomena as in HeLa cells (Fig. S7, ESI†). The spacing is important. Although fluorescence was observed in HepG2 cells just treated with **NI-VD**, it was not as strong as in HeLa cells. After treatment with monensin and nystatin, the fluorescence from HepG2 cells was obviously stronger than that in HeLa cells. The results show that HepG2 cells may be more sensitive to stimuli from monensin and nystatin than HeLa cells. This also illustrated the excellent performance of **NI-VD** that could distinguishing subtle gaps in cell viscosity.

3.6. Fluorescence imaging of *NI-VD* in normal organs, diabetes, and tumor

In the next test, we built some conventional biological models to further evaluate and analyze the performance of **NI-VD**. Diabetes can lead to organ dysfunction and failure [44]. Many recent research reports indicate that one of the causes of diabetic nephropathy is local inflammation caused by cell metabolism disorders [45]. Thus, we built an STZ-induced diabetic mouse model. The kidneys of diabetic mice were dissected and extracted for experiments after confirmation with three consecutive fasting blood glucose tests. Fig. 4 shows that there are differences between the kidneys of normal mice and the diabetic mice by naked eye. The kidneys of the normal mice are bright red and shiny while the kidneys of the model group are slightly yellow and dull. This shows that the model was successfully established. After staining,

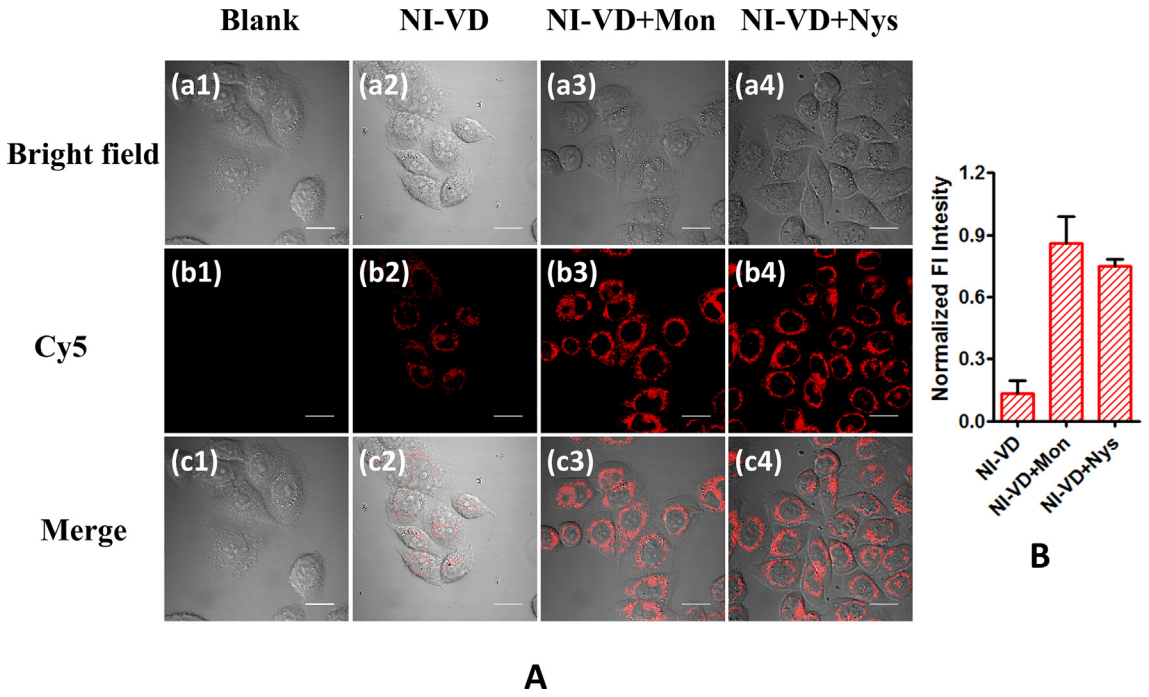

Fig. 3. (A) Fluorescence imaging of HeLa cells. (a1–c1) Images of HeLa cells (a2–c2) Images of HeLa cells stained with 10 μM **NI-VD** for 30 min (a3–c3) HeLa cells exposed to monensin (10 μM), and then incubated with **NI-VD** (10 μM). (a4–c4) Cells pre-treated with nystatin (10 μM), and then treated with **NI-VD** (10 μM). (a1–a4) Bright-field images of HeLa cells. (b1–b4) Fluorescence images of HeLa cells in the red channel (Cy5). (c1–c4) The overlay of the bright-field and red channel. (B) Normalized fluorescence intensity of HeLa cells in OP mode. Conditions: λ_{ex} = 561 nm, λ_{em} = 663–738 nm. Scale bar: 20 μm.

the glomerular podocytes of the model group had slight lesions, and the gap between the cells was enlarged. The swelling of renal tubular epithelial cells was accompanied by vacuolation and a certain degree of deformation. In normal mice, the cells were arranged in an orderly and stable manner. The two kidney types were immersed in the same culture medium with 10 μM **NI-VD** for 30 min. Weak fluorescence was seen in the kidneys of the normal group, and strong fluorescence was seen in the kidneys of the model group. The average fluorescence intensity of the model group was 2.6-times that of the normal group.

The same phenomenon was observed at the cellular level with confocal microscopy (Fig. 5). The fluorescence in model group

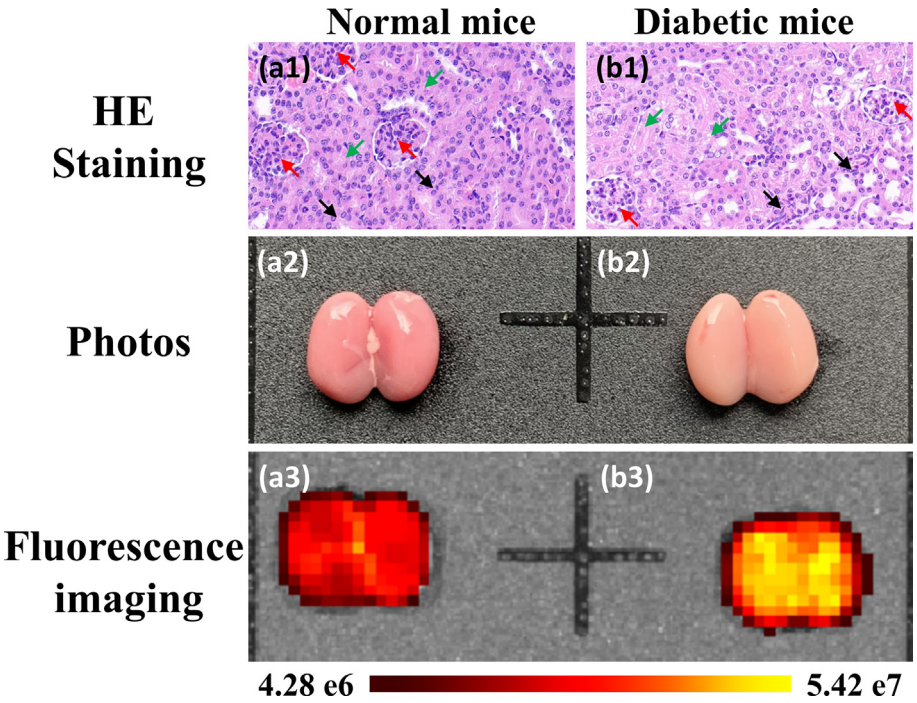

Fig. 4. (a1-a3) Normal mouse group. (b1-b3) Diabetic mouse group. (a1) He staining of normal mouse kidney. (a2) Photo of normal mouse kidney. (a3) Fluorescence imaging of normal mouse kidney with **NI-VD**. (b1) He staining of diabetic mouse kidney. The gap between the cells was enlarged (red arrow), swelling of renal tubular epithelial cells accompanied by vacuolation and a certain degree of deformation (green arrow). (b2) Photo of diabetic mouse kidney. (b3) Fluorescence imaging of normal mouse kidney with **NI-VD**. Conditions: λ_{ex} = 560 nm, λ_{em} = 740 nm.

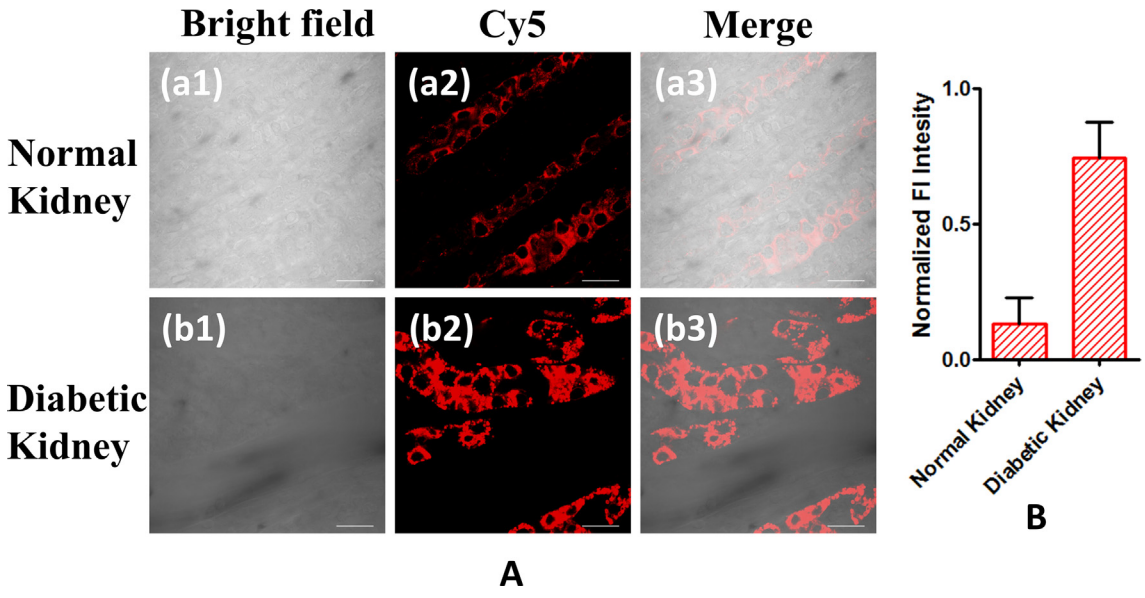

Fig. 5. (A) Fluorescence imaging of kidney tissues stained with **NI-VD**. (a1–a3) Images of normal kidney tissues with 10 μM **NI-VD** for 30 min. (b1–b3) Images of diabetic kidney tissues stained with 10 μM **NI-VD** for 30 min. (a1–b1) Bright-field images of kidney tissues. (a2–b2) Fluorescence images of kidney tissues in the red channel (Cy5). (a3–b3) The overlay of the bright-field and red channel. (B) Normalized fluorescence intensity of kidney tissues in OP mode. Conditions: λ_{ex} = 561 nm, λ_{em} = 663–738 nm. Scale bar: 20 μm.

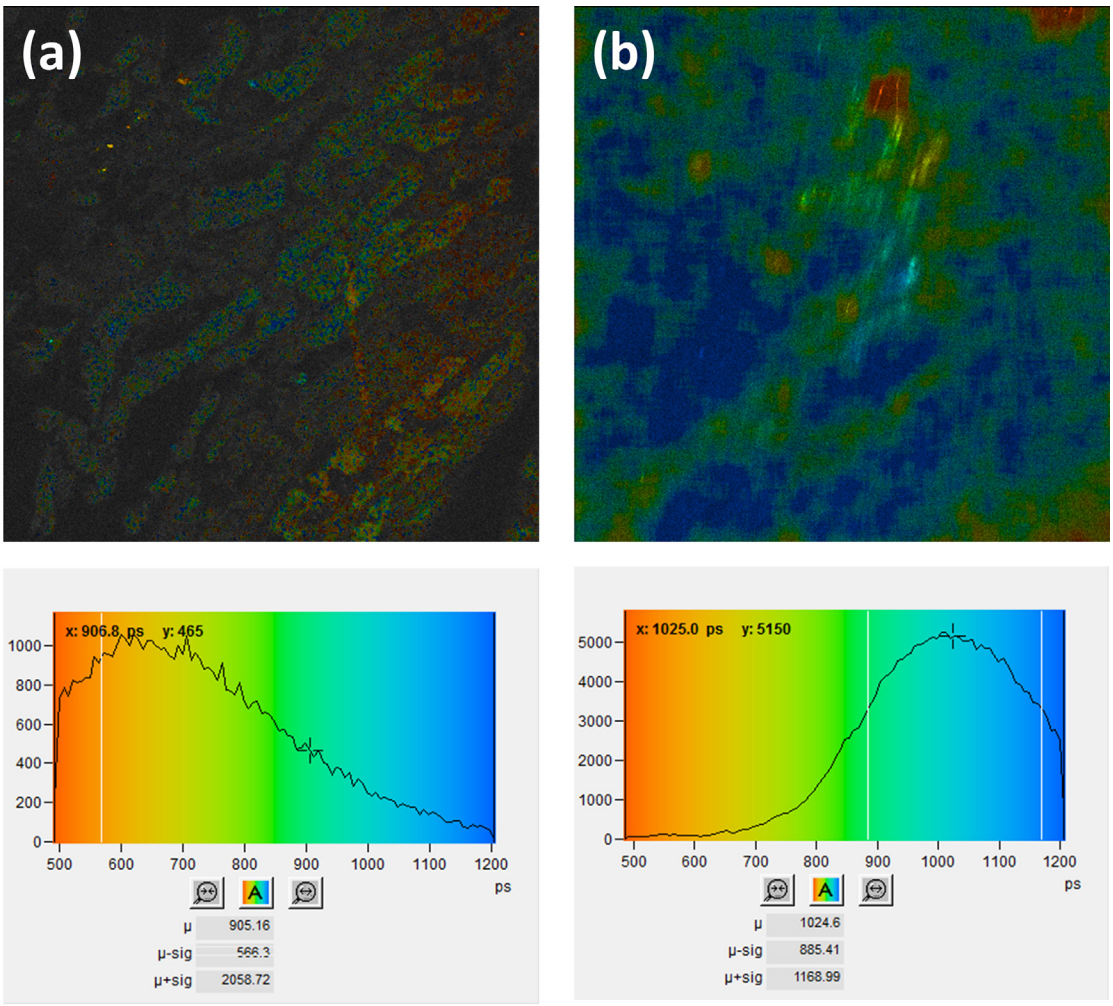

Fig. 6. Fluorescence lifetime imaging of normal kidney and diabetic kidney marked with **NI-VD**. (a) Fluorescence lifetime images of normal kidney tissues. (b) Fluorescence lifetime images of diabetic kidney tissues. Conditions: λ_{ex} = 560 nm, λ_{em} = 740 nm.

was 2.4-times that of the normal group under the same contrast, which indicates that the viscosity of the cells in the kidney would increase after the diabetic model was confirmed.

Through fluorescence lifetime imaging, we further revealed the differences between normal kidney and diabetic kidney. Fig. 6 details the lifetime distribution of **NI-VD** in diseased kidney cells. There are clear differences from normal kidney cells. Fluorescence lifetime imaging has good sensitivity to the detection of viscosity and further confirmed our conclusion.

This is the first report to evaluate changes of viscosity in kidneys with diabetic nephropathy at the cell and tissue levels. We also visualized the viscosity in normal organs and tumor tissues used by **NI-VD**. We carefully removed the heart, liver, spleen, lung, kidneys, and tumor tissues from a tumor model mouse. The organs were washed three times with PBS and placed in PBS with 20 μM **NI-VD**. The treatment was ended after 30 min. Fluorescence in normal organs was dim, while strong fluorescence was observed in tumor tissues. The reason is that the viscosity in tumor cells is larger than in normal cells. (Fig. S8, ESI†) This phenomenon is consistent with previously reported literature. After testing, the penetration depth of **NI-VD** is 30 μM (Fig. S9, ESI†). These data show the application potential of **NI-VD** in the diagnosis and treatment of tumors and diabetic nephropathy.

3.7. Fluorescence imaging of *NI-VD* in zebrafish

The great success of **NI-VD** application in the organization encourages us to plan the next application in living organisms. Zebrafish are a spine model and are extremely popular because of their versatility and ease. We continued the above experiment and continued to stimulate zebrafish with monensin and nystatin to get the same results in living organisms. When the zebrafish were incubated with the **NI-VD** after stimulating with the two drugs above for 30 min (Fig. 7), stronger fluorescence was recorded throughout the zebrafish as expected. Interestingly, we also observed that the average fluorescence intensity increases with time (Fig. S10, ESI†). The fluorescence only adheres to the surface of zebrafish at the beginning and spreads over the whole body with time. The result showed that the **NI-VD** had good tissue permeability. This also proves that **NI-VD** could be a good tool to visualize the viscosity in the mitochondria and apply it to living bodies. This offers more solutions for the diagnosis and treatment of abnormal viscosity in zebrafish.

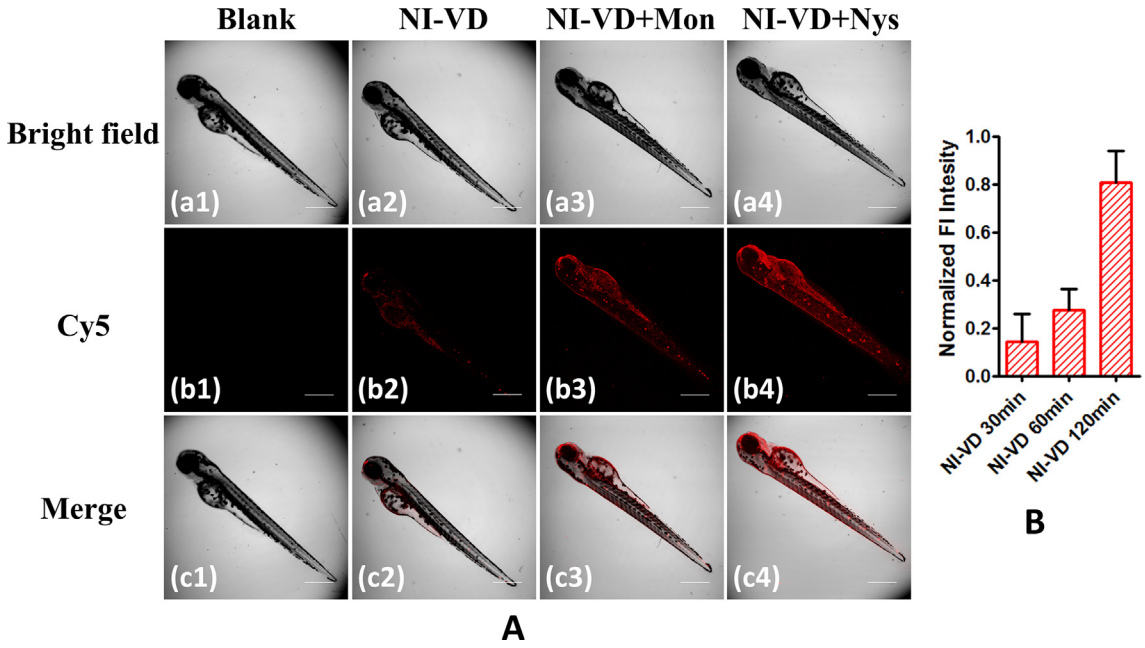

Fig. 7. (A) Fluorescence imaging of zebrafish with **NI-VD** (20 μM). (a1–c1) Images of zebrafish. (a2–c2) Images of zebrafish stained with 10 μM **NI-VD** for 30 min (a3–c3) Zebrafish exposed to monensin (10 μM), and then incubated with **NI-VD** (10 μM). (a4–c4) Zebrafish pre-treated with nystatin (10 μM), and then treated with **NI-VD** (10 μM). (a1–a4) Bright-field images of zebrafish. (b1–b4) Fluorescence images of zebrafish in the red channel (Cy5). (c1–c4) The overlay of the bright-field and red channel. (B) Normalized fluorescence intensity of zebrafish in OP mode. Conditions: λ_{ex} = 561 nm, λ_{em} = 663–738 nm. Scale bar: 20 μm.

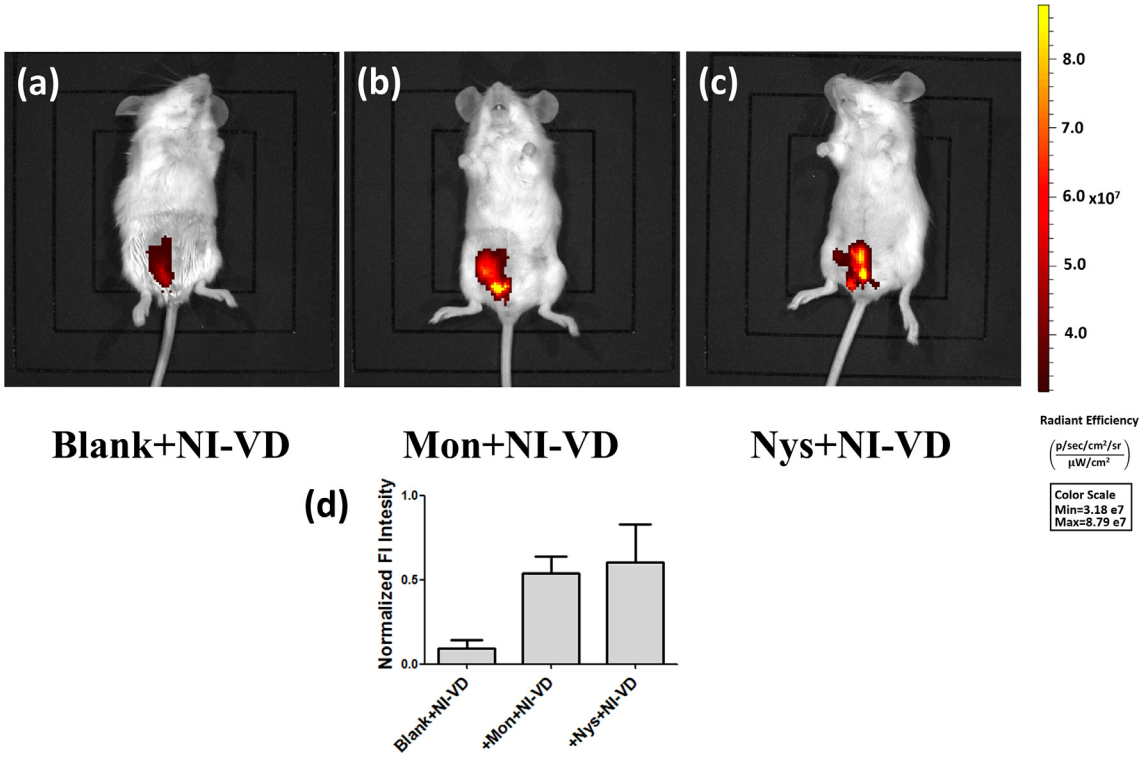

Fig. 8. Fluorescence imaging of living mice. (a) Normal living mice treated with **NI-VD**. (b) Mice treated with **NI-VD** after induce by monensin. (c) Mice treated with **NI-VD** after induce by nystatin. Conditions: λ_{ex} = 560 nm, λ_{em} = 740 nm.

*3.8. Fluorescence imaging of **NI-VD** in mice*

Additional mouse disease models were used to evaluate **NI-VD** in advanced organisms. We induced abnormalities in the mitochondria in the mice via monensin and nystatin and used **NI-VD** to detect the changes of viscosity in the mice. Thirty minutes after intraperitoneal injection of **NI-VD**, the fluorescence intensity of the control group is very weak, but the fluorescence of the model group is very strong (Fig. 8). This result agrees with the cells and zebrafish data. These experiments show that probe **NI-VD** can detect changes in intracellular mitochondrial viscosity.

4. Conclusions

In summary, we report a novel probe that can visualize the distinction diabetic kidney from normal kidney for the first time by monitoring changes in cell viscosity. It verified by each other through cell fluorescence intensity imaging and fluorescence lifetime imaging to make the experimental results true and credible. The synthesis method of **NI-VD** is simple and feasible, the large Stokes' shift, near-infrared emission peak, and specific response imply that **NI-VD** can monitor changes in mitochondrial viscosity at the cell, organ, and organism level. **NI-VD** is a new solution for the diagnosis and treatment of diabetic nephropathy.

Declaration of Competing Interest

The authors declare that they have no known competing financial interests or personal relationships that could have appeared to influence the work reported in this paper.

Acknowledgements

This work was financially supported by NSFC (21672083, and 21877048, 22077048), Taishan Scholar Foundation (TS 201511041), and the startup fund of University of Jinan (309-10004).

Appendix A. Supplementary material

Supplementary data to this article can be found online at https://doi.org/10.1016/j.saa.2021.119627.

References

[1] N. Roopa, V. Kumar, M. Bhalla, Kumar, Development and sensing applications of fluorescent motifs within the mitochondrial environment, Chem. Commun. 51 (2015) 15614–15628.
[2] K. Zheng, W. Lin, L. Tan, H. Chen, H. Cui, A unique carbazole–coumarin fused two-photon platform: development of a robust two-photon fluorescent probe for imaging carbon monoxide in living tissues, Chem. Sci. 5 (2014) 3439–3448.
[3] H. Ren, F. Huo, Y. Zhang, S. Zhao, C. Yin, An NIR ESIPT-based fluorescent probe with large stokes shift for specific detection of Cys and its bioimaging in cells and mice, Sens. Actuators B Chem. 319 (2020) 128248–128256.
[4] N. Ahmed, W. Zareen, D. Zhang, X. Yang, Y. Ye, A DCM-based NIR sensor for selective and sensitive detection of Zn2+ in living cells, Spectrochim. Acta A Mol. Biomol. Spectrosc. 243 (2020) 118758–118764.
[5] Y.-H. Yan, X.-Y. He, J.-Y. Miao, B.-X. Zhao, A near-infrared and mitochondria-targeted fluorescence probe for ratiometric monitoring of sulfur dioxide derivatives in living cells, J. Mater. Chem. B 7 (2019) 6585–6591.
[6] Y. Wu, W. Shu, C. Zeng, B. Guo, J. Shi, J. Jing, X. Zhang, A mitochondria targetable and viscosity sensitive fluorescent probe and its applications for distinguishing cancerous cells, Dyes Pigments 168 (2019) 134–139.
[7] W. Shu, S. Zang, C. Wang, M. Gao, J. Jing, X. Zhang, An endoplasmic reticulum-targeted ratiometric fluorescent probe for the sensing of hydrogen sulfide in living cells and zebrafish, Anal. Chem. 92 (2020) 9982–9988.
[8] M.K. Kuimova, G. Yahioglu, J.A. Levitt, K. Suhling, Molecular rotor measures viscosity of live cells via fluorescence lifetime imaging, J. Am. Chem. Soc. 130 (2008) 6672–6673.
[9] J.A. Dix, A.S. Verkman, Mapping of fluorescence anisotropy in living cells by ratio imaging. Application to cytoplasmic viscosity, Biophys. J. 57 (1990) 231–240.
[10] K. Luby-Phelps, S. Mujumdar, R.B. Mujumdar, L.A. Ernst, W. Galbraith, A.S. Waggoner, A novel fluorescence ratiometric method confirms the low solvent viscosity of the cytoplasm, Biophys. J. 65 (1993) 236–242.
[11] M.K. Kuimova, S.W. Botchway, A.W. Parker, M. Balaz, H.A. Collins, H.L. Anderson, K. Suhling, P.R. Ogilby, Imaging intracellular viscosity of a single cell during photoinduced cell death, Nat. Chem. 1 (2009) 69–73.
[12] Z. Yang, Y. He, J.H. Lee, N. Park, M. Suh, W.S. Chae, J. Cao, X. Peng, H. Jung, C. Kang, J.S. Kim, A self-calibrating bipartite viscosity sensor for mitochondria, J. Am. Chem. Soc. 135 (2013) 9181–9185.
[13] H.P. Kao, J.R. Abney, A.S. Verkman, Determinants of the translational mobility of a small solute in cell cytoplasm, J. Cell Biol. 120 (1993) 175–184.
[14] M.J. Hansson, S. Morota, M. Teilum, G. Mattiasson, H. Uchino, E.J. Elmer, Increased potassium conductance of brain mitochondria induces resistance to permeability transition by enhancing matrix volume, J. Biol. Chem. 285 (2010) 741–750.
[15] Y. Zhang, J. Wang, P. Jia, X. Yu, H. Liu, X. Liu, N. Zhao, B. Huang, Two-photon fluorescence imaging of DNA in living plant turbid tissue with carbazole dicationic salt, Org. Biomol. Chem. 8 (2010) 4582–4588.
[16] B.F. Zhang, L. Xing, P.F. Cui, F.Z. Wang, R.L. Xie, J.L. Zhang, M. Zhang, Y.J. He, J.Y. Lyu, J.B. Qiao, B.A. Chen, H.L. Jiang, Mitochondria apoptosis pathway synergistically activated by hierarchical targeted nanoparticles co-delivering siRNA and lonidamine, Biomaterials 61 (2015) 178–189.
[17] M. Ren, K. Zhou, L. Wang, K. Liu, W. Lin, Construction of a ratiometric two-photon fluorescent probe to monitor the changes of mitochondrial viscosity, Sens. Actuators B Chem. 262 (2018) 452–459.
[18] B. Calvignac, E. Rodier, J.-J. Letourneau, P. Vitoux, C. Aymonier, J. Fages, Development of an improved falling ball viscometer for high-pressure measurements with supercritical CO2, J. Supercrit. Fluid 55 (2010) 96–106.
[19] R.F. Berg, E.F. May, M.R. Moldover, Viscosity ratio measurements with capillary viscometers, J. Chem. Eng. Data 59 (2014) 116–124.
[20] C. Casaretto, M. Martínez Sarrasague, S. Giuliano, E. Rubin de Celis, M. Gambarotta, I. Carretero, M. Miragaya, Evaluation of Lama glama semen viscosity with a cone-plate rotational viscometer, Andrologia 44 (2012) 335–341.
[21] Z. Yang, J. Cao, Y. He, J.H. Yang, T. Kim, X. Peng, J.S. Kim, Macro-/micro-environment-sensitive chemosensing and biological imaging, Chem. Soc. Rev. 43 (2014) 4563–4601.
[22] B. Guo, J. Jing, L. Nie, F. Xin, C. Gao, W. Yang, X. Zhang, A lysosome targetable versatile fluorescent probe for imaging viscosity and peroxynitrite with different fluorescence signals in living cells, J. Mater. Chem. B 6 (2018) 580–585.
[23] X. Zhang, Q. Sun, Z. Huang, L. Huang, Y. Xiao, Immobilizable fluorescent probes for monitoring the mitochondria microenvironment: a next step from the classic, J. Mater. Chem. B 7 (2019) 2749–2758.
[24] J. Kizhakekuttu Tinoy, J. Wang, K. Dharmashankar, R. Ying, D. Gutterman David, A. Vita Joseph, E. Widlansky Michael, Adverse alterations in mitochondrial function contribute to type 2 Diabetes mellitus-related endothelial dysfunction in humans, Arterioscler. Thromb. Vasc. Biol. 32 (2012) 2531–2539.
[25] J. Wang, A. Alexanian, R. Ying, J. Kizhakekuttu Tinoy, K. Dharmashankar, J. Vasquez-Vivar, D. Gutterman David, E. Widlansky Michael, Acute exposure to low glucose rapidly induces endothelial dysfunction and mitochondrial oxidative stress, Arterioscler. Thromb. Vasc. Biol. 32 (2012) 712–720.
[26] A. El-Osta, D. Brasacchio, D. Yao, A. Pocai, P.L. Jones, R.G. Roeder, M.E. Cooper, M. Brownlee, Transient high glucose causes persistent epigenetic changes and altered gene expression during subsequent normoglycemia, J. Exp. Med. 205 (2008) 2409–2417.
[27] M. Brownlee, Biochemistry and molecular cell biology of diabetic complications, Nature 414 (2001) 813–820.
[28] J.M. Forbes, D.R. Thorburn, Mitochondrial dysfunction in diabetic kidney disease, Nat. Rev. Nephrol. 14 (2018) 291–312.
[29] T. Eleftheriadis, G. Pissas, G. Antoniadi, V. Liakopoulos, I. Stefanidis, Allopurinol protects human glomerular endothelial cells from high glucose-induced reactive oxygen species generation, p53 overexpression and endothelial dysfunction, Int. Urol. Nephrol. 50 (2018) 179–186.
[30] J.J. Chen, B.P. Yu, Alterations in mitochondrial membrane fluidity by lipid peroxidation products, Free Radic. Biol. Med. 17 (1994) 411–418.
[31] J.J. García, L. López-Pingarrón, P. Almeida-Souza, A. Tres, P. Escudero, F.A. García-Gil, D.-X. Tan, R.J. Reiter, J.M. Ramírez, M. Bernal-Pérez, Protective effects of melatonin in reducing oxidative stress and in preserving the fluidity of biological membranes: a review, J. Pineal Res. 56 (2014) 225–237.
[32] L. Yuan, W. Lin, S. Zhao, W. Gao, B. Chen, L. He, S. Zhu, A unique approach to development of near-infrared fluorescent sensors for in vivo imaging, J. Am. Chem. Soc. 134 (2012) 13510–13523.
[33] R. Feng, L. Guo, J. Fang, Y. Jia, X. Wang, Q. Wei, X. Yu, Construction of the FRET Pairs for the visualization of mitochondria membrane potential in dual emission colors, Anal. Chem. 91 (2019) 3704–3709.
[34] X.-H. Xu, C. Liu, Y. Mei, Q.-H. Song, BODIPY-based selenides as fluorescent probes for rapid, sensitive and mitochondria-specific detection of hypochlorous acid, J. Mater. Chem. B 7 (2019) 6861–6867.
[35] W. Shu, Y. Wu, S. Zang, S. Su, H. Kang, J. Jing, X. Zhang, A mitochondria-targeting highly specific fluorescent probe for fast sensing of endogenous peroxynitrite in living cells, Sens. Actuators B Chem. 303 (2020) 127284–127291.
[36] L. Yu, J.F. Zhang, M. Li, D. Jiang, Y. Zhou, P. Verwilst, J.S. Kim, Combining viscosity-restricted intramolecular motion and mitochondrial targeting leads to selective tumor visualization, Chem. Commun. 56 (2020) 6684–6687.
[37] Y. Zhang, Z. Li, W. Hu, Z. Liu, A Mitochondrial-targeting near-infrared fluorescent probe for visualizing and monitoring viscosity in live cells and tissues, Anal. Chem. 91 (2019) 10302–10309.
[38] J. Yue, Y. Shen, L. Liang, L. Cong, W. Xu, W. Shi, C. Liang, S. Xu, Revealing mitochondrial microenvironmental evolution triggered by photodynamic therapy, Anal. Chem. 92 (2020) 6081–6087.
[39] K. Wang, S. Ma, Y. Ma, Y. Zhao, M. Xing, L. Zhou, D. Cao, W. Lin, Aurone derivative revealing the metabolism of lipid droplets and monitoring oxidative stress in living cells, Anal. Chem. 92 (2020) 6631–6636.
[40] L. Dai, M. Ren, Z. Li, L. Wang, W. Lin, A targetable fluorescent probe for imaging of mitochondrial viscosity in living cells, Anal. Methods 11 (2019) 4561–4565.
[41] K. Liu, Y. Chen, H. Sun, S. Wang, F. Kong, Construction of a novel near-infrared fluorescent probe with multiple fluorescence emission and its application for

SO2 derivative detection in cells and living zebrafish, J. Mater. Chem. B 6 (2018) 7060–7065.
[42] K. Dou, W. Huang, Y. Xiang, S. Li, Z. Liu, Design of activatable NIR-II molecular probe for in vivo elucidation of disease-related viscosity variations, Anal. Chem. 92 (2020) 4177–4181.
[43] W. Shu, Y. Wu, T. Shen, J. Cui, H. Kang, J. Jing, X. Zhang, A mitochondria-targeted far red fluorescent probe for ratiometric imaging of endogenous peroxynitrite, Dyes Pigments 170 (2019) 107609–107614.
[44] X. Ding, T. Jian, Y. Wu, Y. Zuo, J. Li, H. Lv, L. Ma, B. Ren, L. Zhao, W. Li, J. Chen, Ellagic acid ameliorates oxidative stress and insulin resistance in high glucose-treated HepG2 cells via miR-223/keap1-Nrf2 pathway, Biomed. Pharmacother. 110 (2019) 85–94.
[45] F.Y. Chow, D.J. Nikolic-Paterson, E. Ozols, R.C. Atkins, G.H. Tesch, Intercellular adhesion molecule-1 deficiency is protective against nephropathy in Type 2 diabetic db/db mice, J. Am. Soc. Nephrol. 16 (2005) 1711–1722.